Thermal transport in graphene supported on copper

Liang Chen[a] and Satish Kumar[a]
G.W. Woodruff School of Mechanical Engineering, Georgia Institute of Technology, Atlanta, Georgia 30318, USA

(Received 10 March 2012; accepted 2 July 2012; published online 16 August 2012)

We investigate the thermal transport in isolated single layer graphene (SLG) and SLG supported on Cu substrate using equilibrium molecular dynamics simulations and relaxation time approximation (RTA) method. We observe significant changes in the SLG dispersion curve in low frequency and low wave-vector region due to the interaction with Cu substrate. Several new phonon modes related to out-of-plane vibrations appear at the low frequency and small wave vector regions, but their contribution to graphene thermal conductivity is negligible. The thermal conductivity of graphene decreases by 44% due to the interactions with Cu substrate for high interaction strength parameter in Lennard-Jones potential formulation for graphene-Cu interaction. The phonon mode analysis through the RTA approach shows that the acoustic phonons dominate the thermal transport for both isolated and supported graphenes. The longitudinal acoustic (LA), transverse acoustic (TA), and out-of-plane acoustic (ZA) phonons contribute 654, 330, and 361 W/mK to the lattice thermal conductivity of isolated graphene, respectively. The phonon life time of ZA modes decreases by order of magnitude due to the interactions with Cu substrate and ZA mode contribution to SLG thermal conductivity decreases by 282 W/mK, while the contributions of LA and TA phonons reduce by 77.4 W/mK and 82.9 W/mK, respectively.
[http://dx.doi.org/10.1063/1.4740071]

I. INTRODUCTION

The exceptional electronic[1,2] and mechanical properties of graphene have made it a very promising nano-material for future electronic applications.[3,4] The high electron mobility or thermal conductivity of graphene is of great interest for the radio frequency devices, interconnects, and thermal management of electronic devices.[5,6] The thermal conductivity of suspended single layer graphene (SLG) was measured to be as high as 3000–5300 W/mK.[6–8] Recent measurements show high thermal conductivity of suspended SLG grown by chemical vapor deposition (CVD) technique, e.g., 2500 W/mK at 350 K and 1400 W/mK at about 500 K.[9] However, graphene-substrate interactions can significantly reduce the thermal conductivity of the supported SLG[3] and the supported few-layer graphene.[10] The thermal conductivity of SLG supported on SiO_2 was measured as 600 W/mK at room temperature, which is much lower than the suspended SLG but still considerably higher than many metals ($\sim$Cu) typically used in the electronic devices.[3] As graphene will be either supported or embedded in most of the applications such as field effect transistors or interconnects, a good understanding of the graphene thermal interaction with different materials such as dielectrics ($\sim SiO_2$) and metals (Cu, Au, and Pd) is crucial. The contact with metals is extremely important and unavoidable in the graphene based nanoelectronics, e.g., in graphene-based field effect transistors (FETs), a graphene layer connects the source and drain electrodes which are typically made of metals. Recently, the importance of Joule heating, current crowding, and thermoelectric effects has been explored at graphene-metal contact.[11–13] Thermal transport at graphene-metal contact becomes particularly important in short channel transistors where the electrode contact can turn into a crucial heat removal pathway.[14,15] Graphene-metal contacts cannot be avoided in graphene and Cu based interconnects in very large scale integrated (VLSI) circuits.[16] At high temperatures, graphene interconnects may become an important channel to spread heat inside an electronic package.[17] The metal contacts can significantly change the thermal properties of graphene. In spite of such crucial importance of the graphene-metal contact, the effect of metal substrate on graphene thermal properties has not been well explored.

Like other carbon allotropes including diamond, graphite, and carbon nanotubes (CNTs), the thermal transport in graphene is mainly contributed by phonons rather than electrons because of the strong covalent bonding of light carbon atoms.[3,7] The lattice thermal conductivity of isolated graphene has been estimated by recent studies using molecular dynamics (MD) simulations,[18–22] Boltzmann transport equation (BTE) calculations,[23–26] and simplified analytical models.[27–29] A large variation in the SLG thermal conductivity estimation has been observed among these different methods. Non-equilibrium MD simulations generally estimate small values for thermal conductivity because of the boundary scattering.[19–22] The values determined by BTE calculations are comparable with the measurements, but a significant discrepancy exists in the role of the out-of-plane acoustic (ZA) phonons.[3,4,23,26,30,31] Nika *et al.*[25,29] found that the contribution of ZA phonons is negligible due to the large Gruneisen parameter and small group velocity. More recent BTE studies, which include both the normal and Umklapp scattering process, have demonstrated that the out-of-plane acoustic (ZA) modes could dominate the

[a]Authors to whom correspondence should be addressed. Electronic addresses: lchen64@gatech.edu and satish.kumar@me.gatech.edu.

thermal transport in suspended SLG.[3,23,26] The dominant contribution from ZA modes can be attributed to the large density of flexural phonons associated with the quadratic ZA branch dispersion and the restricted phase space for the ZA phonon scattering due to the reflection symmetry of two-dimensional graphene.[23] For supported SLG or multilayer graphene, the substrate coupling or interlayer coupling breaks the reflection symmetry and results in a significant suppression of ZA phonons as well as significant reduction in their thermal conductivity contribution. An analytical model for substrate scattering has to be incorporated in BTE simulations to estimate the effects of substrate. It is hard to incorporate the effect of interfacial structures on interfacial thermal transport using BTE methods. MD simulations can include the substrate structure and substrate scattering effect in a better way as different interfacial atomic configurations can be easily considered and phonon-phonon scattering events at interface including anharmonic effects can be inherently treated in a natural way.

In the present study, we investigate the thermal transport in suspended SLG and SLG supported on Cu using molecular dynamics and relaxation time approximation (RTA) approach at room temperature ($\sim$300 K). We use the equilibrium molecular dynamics (EMD) simulations and Green-Kubo method in order to reduce the finite size and boundary effects that are concerns of non-equilibrium molecular dynamics (NEMD) simulations. The classical MD simulations have some discrepancy with BTE studies in prediction of thermal conductivity as quantum effects are neglected in MD studies. However, the focus of this work is to explore thermal coupling between the SLG and Cu substrate, and MD simulations is an appropriate method to study this coupling as the phonon scattering at the interface dominate the thermal transport of supported SLG and the effect of Cu substrate can be effectively incorporated in MD simulations. We compare the thermal conductivity and dispersion curves of isolated SLG against that of Cu supported SLG. We observe significantly changes in dispersion curve in low frequency and low wavevector regions due to the substrate interactions. We obtain the lifetime of each phonon mode by fitting the spectral energy density (SED) to the Lorentzian function, and calculate the corresponding contribution to thermal conductivity using the RTA approach. Our calculations suggest that longitudinal acoustic (LA) phonons have the largest contribution of 40% to the thermal conductivity of isolated SLG while transverse acoustic (TA) and ZA phonons contribute 20% and 22%, respectively. The thermal conductivity of ZA phonons is reduced by 78% for the SLG supported on Cu, while the thermal conductivities of LA and TA phonons decrease by 12% and 25%, respectively. The absolute value of the reduction in LA and TA phonons contribution to thermal conductivity (77.4 and 82.9 W/mK) is still comparable to that of ZA phonons (282 W/mK) because of their large contribution in isolated SLG.

II. SIMULATION SETUP AND METHODOLOGY

In the MD simulation, the most stable configuration of graphene on the Cu substrate[32,33] is used. As shown in Fig. 1, the SLG honeycomb lattice is positioned to match the triangular lattice of Cu (111) surfaces with one carbon atom on top of a Cu atom (A site) and the second carbon on a hollow site. Since, the Cu substrate is usually much thicker than the SLG, the lattice constant of SLG will tend to match Cu.[32] Therefore, we use the experimentally measured FCC lattice constant of copper (3.61 Å), and adapt the lattice constant of SLG. The lattice constant of SLG is increased by 2.4% (compared to 2.492 Å calculated using the optimized Tersoff potential[19]) to match the Cu lattice. The dimension of the Cu substrate used in the simulation is 60 Å $\times$ 60 Å $\times$ 12.5 Å.

We use LAMMPS package[22] for the molecular dynamics simulations. The optimized Tersoff potential[19] and embedded-atom method (EAM) potential[34] are used to describe the C-C interactions and Cu-Cu interactions, respectively. The optimized Tersoff potential can give improved fits to the three acoustic phonon branches of graphene dispersion curve which play the most important role in the thermal transport in SLG. The van der Waals interaction between C and Cu atoms at the interface is modeled by Lennard-Jones (L-J) potential, $V_{ij}(r) = 4\chi\varepsilon_{ij}[(\sigma_{ij}/r)^{12} - (\sigma_{ij}/r)^{6}]$. The present study employs the L-J parameterization used by Xu and Buehler,[35] with $\varepsilon = 25.78$ meV and $\sigma = 3.0825$ Å. Graphene may have strong interaction and bonding with some metals such as Ti or Ni, but weakly interact with Cu, which justifies the application of L-J potential for Cu-C interaction. We use the parameter χ to adapt the interaction strength between C and Cu atoms.[36] A time step of 0.5 fs is used in all the simulations.

A. Green-Kubo method

In the equilibrium simulation, the system is always in the linear response regime, and the Green-Kubo method can be used to calculate transport coefficients. The thermal conductivity is related to the equilibrium current-current autocorrelation function by the Green-Kubo expression[37]

$$k_{\alpha\beta}(\tau_m) = \frac{1}{Vk_BT^2}\int_0^{\tau_m}\langle J_\alpha(\tau)J_\beta(\tau)\rangle d\tau, \tag{1}$$

where V is the system volume, k_B is the Boltzmann constant, and $J_\alpha(\tau)$ is the heat flux in x, y, or z direction. Periodic boundary conditions are employed in both x and y directions (see Fig. 1(a)) and the thermal conductivity in x and y directions (k_{xx} and k_{yy}) is averaged to calculate the in-plane thermal conductivity of SLG. The Green-Kubo method generally needs a very long simulation time to sufficiently converge the current-current autocorrelation function. In this study, we sample the heat flux every 5 fs and calculate the heat flux autocorrelation using simulation data of 50 ns, which has been observed to sufficiently long to achieve the convergence.

The general expression to calculate the heat flux is $\vec{J}(t) = \frac{d}{dt}\sum_i \vec{r}_i E_i$, where E_i is the total energy of an atom. For the three-body Tersoff potential, it can be expanded as[37]

$$\vec{J}(t) = \sum_i \vec{v}_i\varepsilon_i + \frac{1}{2}\sum_{i,j}(\vec{F}_{ij}\cdot\vec{v}_i)\vec{r}_{ij} + \frac{1}{6}\sum_{i,j,k}(\vec{F}_{ijk}\cdot\vec{v}_i)(\vec{r}_{ij}+\vec{r}_{ik}). \tag{2}$$

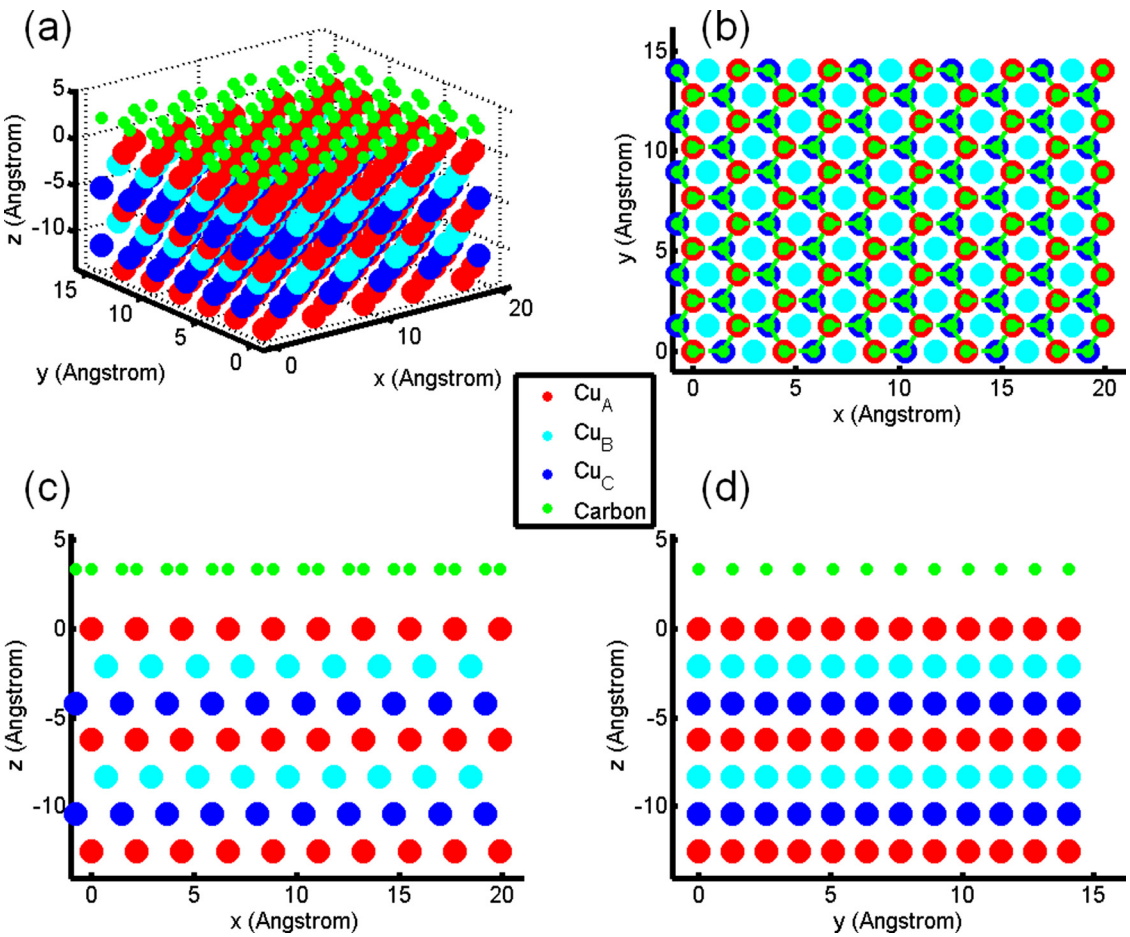

FIG. 1. Schematic diagram of the single layer graphene and Cu-111 system. (a) 3D view; (b) x-y plane; (c) x-z plane; (d) y-z plane. (a)–(d) share the same legend.

The first term is associated with convection, and the second and third with conduction.[38] For a solid system without convection, the first term can be neglected.[39,40]

B. Relaxation time approximation approach

The anisotropic thermal conductivity ($k_{\alpha\beta}$) can be calculated considering relaxation time approximation[25,41]

$$k_{\alpha\beta} = \frac{1}{V}\sum_{s,\vec{q}} \tau(s,\vec{q}) v_\alpha(s,\vec{q}) v_\beta(s,\vec{q}) C_{ph}(\omega_s). \tag{3}$$

Here, v and τ are the phonon group velocity and lifetime, respectively. C_{ph} is the specific heat of a phonon mode of frequency ω

$$C_{ph}(\omega) = \hbar\omega \frac{dN^0}{dT} = \frac{(\hbar\omega)^2}{k_B T^2} \frac{\exp(\hbar\omega/k_B T)}{[\exp(\hbar\omega/k_B T) - 1]^2}. \tag{4}$$

The averaged thermal conductivity of SLG is determined by performing integration in the cylindrical coordinates using the dispersion along Γ-M direction while neglecting the anisotropy of the phonon dispersion[25]

$$k = \frac{1}{4\pi t}\sum_s \int_{q_{\min,s}}^{q_{\max,s}} v_s(q)^2 \tau(s,q) C_{ph}(\omega_s) q dq. \tag{5}$$

Here, t =3.35 Å is the thickness of the SLG.

The phonon group velocities are calculated from the phonon dispersion relations predicted using SED, $v(s,q) = \partial\omega_s/\partial q$. The SED of each branch at certain wave vector and frequency is determined by[42]

$$\Phi(q,\omega,s) = \frac{1}{4\pi\tau_0 N}\sum_\alpha \sum_b^B m_b |e_s \begin{pmatrix} q\omega \\ \alpha b \end{pmatrix} \int_0^{\tau_0} \sum_{n_{x,y}}^N \dot{u}_\alpha(n_{x,y}, b, t) \times \exp\left[i\vec{q}\cdot\vec{r}\begin{pmatrix} n_{x,y} \\ 0 \end{pmatrix} - i\omega_s t \right] dt|^2, \tag{6}$$

where α and b are the subscripts for direction and basis atom in a unit cell. $n_{x,y}$ is the index for unit cell and $\vec{r}_0(n_{x,y})$ is the equilibrium position of each unit cell. e_s is the polarization vector of the basis atom b for the phonon branch α at wavevector q. We incorporate the effect of phonon polarization vector in the calculation of mode dependent SED which has been neglected in the previous studies.[42] It is obtained from the harmonic lattice dynamics calculations using the GULP[21] code with optimized Tersoff potential. The phonon lifetime ($\tau = 1/2\gamma$) is obtained by fitting the SED to the Lorentzian function as[42]

$$\Phi(q,\omega,s) = \frac{I}{1 + [(\omega - \omega_c)/\gamma]^2}, \tag{7}$$

where I is the magnitude of the SED peak, ω_c is the peak center frequency, and γ is the half-width at half-maximum. In this method, the full anharmonicity of the atomic interactions can be incorporated into the prediction of phonon lifetime and dispersion relations. The scattering of phonons at the interface with substrate due to the nonperiodic interactions can also be taken into account.

III. RESULTS AND DISCUSSION

A. Isolated graphene

The thermal conductivity of isolated SLG is computed using Green-Kubo method described in Sec. II. In order to achieve a good ergodicity of the phonon phase space, four independent simulations are performed for each case using different initial velocities of atoms following Gaussian distribution. The computed thermal conductivity of the isolated SLG is shown in Fig. 2. A good convergence can be achieved by averaging over just four independent simulations as shown in Fig. 2. The thermal conductivity is obtained by averaging over a smooth region once the integral of heat flux autocorrelation function converges to constant values (red solid circles in Fig. 2).[43]

NEMD simulations use heat source and sink which bring the size effect in the thermal conductivity calculations. The size effect in Green-Kubo method is much less severe than that in NEMD (Ref. 44) as periodic boundaries are employed. However, the size effects still play a role in Green-Kubo method as for a system with very small size all long-wavelength phonon modes may not get excited which may have important contribution to phonon thermal conductivity.[4,8,18,31,37] Our calculations using Green-Kubo method also indicate size dependent thermal conductivity of SLG. The thermal conductivity of 30×30 Å SLG is estimated as 2520 W/mK, which is close to the thermal conductivity obtained from MD simulations in previous studies on the SLG of similar size.[8,45] The thermal conductivity is observed to decrease with increasing simulation domain of SLG when the size is small. This trend is just opposite to what is typically observed for graphene nano-ribbon or systems with fixed boundaries in NEMD simulations. While using Green-Kubo method for the SLG with periodic boundary condition, phonons may pass the system several times without scattering,[37] which is particularly more frequent for the small systems. In the absence of external scattering mechanism (e.g., defect scattering, impurity scattering, and boundary scattering), only few three-phonon U-process exists for long wave length phonons. The number of excited phonon modes may be limited for the MD simulation with a small domain, and some long wave length phonons (phonons with wave length comparable to the system size) encounter few scattering event and travel ballistically, resulting in a large artificial thermal conductivity.[31] More phonon modes are excited with increasing system size but phonon-phonon scattering also increases.[18] Because of this trade-off, the thermal conductivity values saturate once the size of SLG approaches 200×200 Å. However, the effect of decreasing SLG size on its thermal conductivity significantly reduces once SLG becomes larger than 60×60 Å. The computation is much more expensive for SLG supported on Cu (111) substrate due to the presence of thick Cu substrate. The SLG of 60×60 Å size is selected for the simulations of Cu supported SLG considering the trade-off between the eliminating size effect and reducing computational efforts. We use modified Tersoff potential parameters for all MD simulations, but we also tested the original Tersoff parameters[46] using Green-Kubo method which estimates a much smaller thermal conductivity of 541 W/mK for the 60×60 Å SLG compared to 1606 W/mK using modified Tersoff potential parameters.

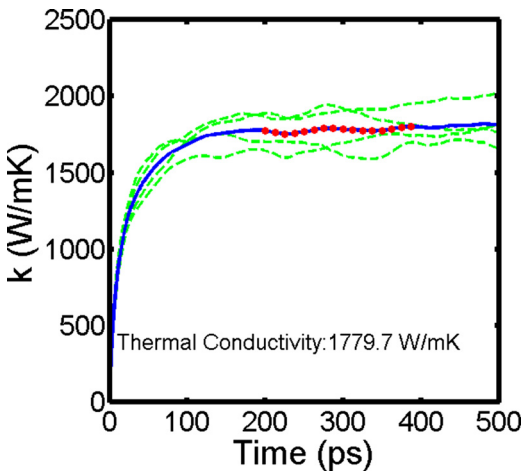

FIG. 2. Thermal conductivity of isolated SLG of size 60×60 Å obtained from the integral of heat flux autocorrelation function (see Eq. (1)). The blue solid line is the average of four independent simulations (green dotted lines). The thermal conductivity is obtained by averaging the region marked by red solid circles.

B. Graphene supported on Cu (111)

Large oscillations in the heat current auto-correlation function occur when atoms of different atomic masses are present at the interface which makes evaluation of the HCACF integral relatively difficult. To address these oscillations and convergence issues in our simulations for supported SLG, we employ the approach followed in Ref. 40, i.e., neglect the convection term in the heat flux calculations. Large oscillations in the HCACF can be eliminated using this method as shown in Fig. 3(a). The convection term is also neglected for the isolated SLG. Only a small deviation in thermal conductivity is observed by neglecting convection term, e.g., less than 6% for isolated SLG of size 60×60 Å. By comparing Figs. 2(a) and 3(a), we can observe that the integral of HCACF converges faster for the supported SLG than the isolated SLG. This indicates that the lifetime of certain phonon modes is shortened due to the scattering with substrate, and the corresponding contribution to HCACF and thermal conductivity is suppressed.

By varying the interaction strength factor χ in the L-J potential, we investigate the effects of C-Cu coupling strength on the thermal conductivity. As shown in Figure 3(b), the point at $\chi = 0$ corresponds to the isolated SLG. The interactions with substrate result in 28% reduction of the SLG thermal conductivity using standard L-J parameters ($\chi = 1$) for the SLG-Cu (111) system. Thermal conductivity

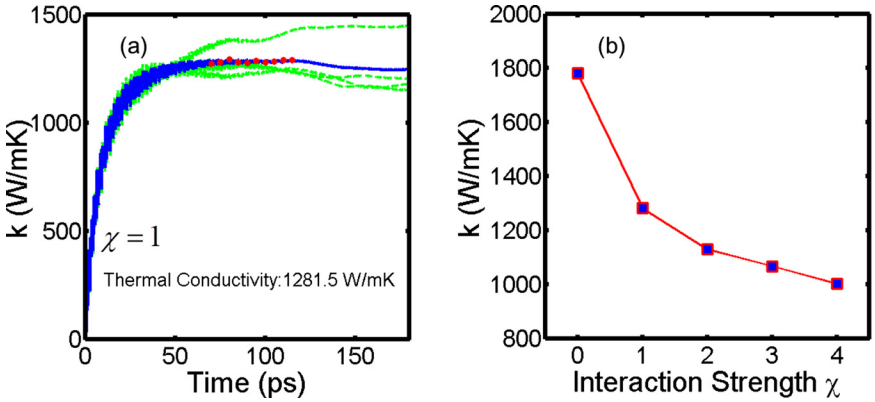

FIG. 3. (a) Thermal conductivity obtained from the integral of heat flux autocorrelation function of Cu-supported SLG (60×60 Å). The blue solid line is the average of four independent simulations (green dotted lines). The thermal conductivity is obtained by averaging the region marked by red solid circles; (b) variations of thermal conductivity with the L-J interaction strength factor χ between C and Cu atoms.

of SLG further reduces with increasing χ, but the rate of decrease slows down. A further reduction of 16% is observed ($\sim$total 44%) when the interaction strength factor χ is increased from 1 to 4. This reduction in thermal conductivity is smaller than the recent experimental results on graphene supported on SiO_2 substrate.[3] This may be due to two reasons: (1) the relatively smooth Cu (111) surface leads to less interface scattering of phonons; (2) neglect of quantum effects and the deviation of phonon distribution by the classical MD simulations. To further understand this, we next analyze the contribution of different phonon modes to the thermal transport in SLG using RTA method and explore the effect of thermal interactions at SLG-Cu interface.

C. Contributions of different phonon modes

Some recent studies investigate the thermal transport in the SLG and multi-layer graphene using BTE based methods. The contribution from different phonon modes has been presented and the importance of appropriately considering the selection rules has been demonstrated.[23,26] However, the role of phonon modes in the thermal transport of SLG supported on Cu substrate has not yet been quantitatively studied. In this section, we predict the dispersion relations and phonon lifetime by means of SED using the velocities from equilibrium MD simulations, and then calculate the contribution of different phonon modes to thermal conductivity using RTA method.

Figure 4 shows the dispersion curves of isolated SLG and Cu supported SLG, which is estimated from the contour plot of the sum of SED, $\Phi(q, \omega, s)$, of each mode. The $\Phi(q, \omega, s)$ is averaged over 20 independent simulations to mitigate the inherent fluctuation in MD simulation results. The black solid lines in Fig. 4(a) correspond to dispersion curves made by connecting the peaks of SED of each mode. By comparing Figs. 4(a) and 4(b), we can observe that the substrate interactions do not have an obvious effect on the LA, TA, and the three optical phonon modes. However, the ZA modes have been significantly changed due to the substrate interactions. Several modes related to out-of-plane vibrations appear at the low frequency and small wave vector region ($\sim$dimensionless wave vector $q* = q/q_M < 0.5$), as marked by the yellow dashed rectangle and the inset in Figure 4(b). These modes with non-zero frequency at Γ point are similar to the layer-breathing mode in bilayer graphene and graphite.[28] They correspond to the out-of-phase vibration of C-Cu atom pair in direction perpendicular to graphene-Cu interface. References 27 and 29 suggested that there exists a cut-off frequency below which the coupling with the substrate phonons and cross-plane phonons becomes strong in the supported SLG or graphite. As a result, the phonon energy leaks to the substrate and the contributions of these low frequency phonons to the in-plane thermal transport are reduced to negligible. The blurred region in Fig. 3(b) indicates a cut-off frequency of 6 THz for the ZA phonon modes in SLG supported on Cu. Since the ZA phonons have a maximum frequency of 14 THz at M point, this cut-off frequency has covered ZA phonon modes with $q^* \leq 0.5$, i.e., 50% of the allowed ZA phonon modes in Γ-M direction.

Figure 5 shows the semilogarithmic plot of SED versus frequency along the Γ-M direction at $q^* = 2/14$ for the isolated and supported SLGs. The corresponding fitting curves to Lorentzian function are also presented in this figure. The SED at the other wave vectors has similar peak-and-valley

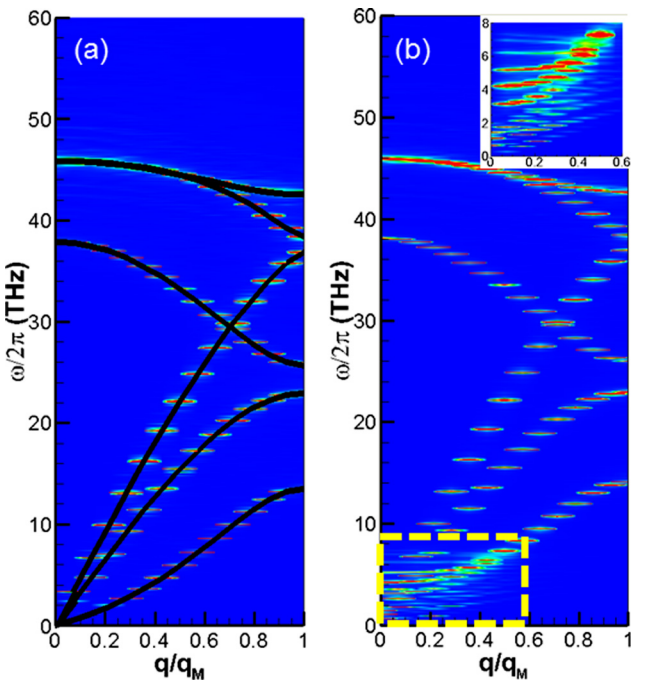

FIG. 4. Phonon dispersion curves (a) isolated single layer graphene (SLG) and (b) SLG supported on Cu (111). The inset of (b) shows details of the low frequency region of ZA modes.

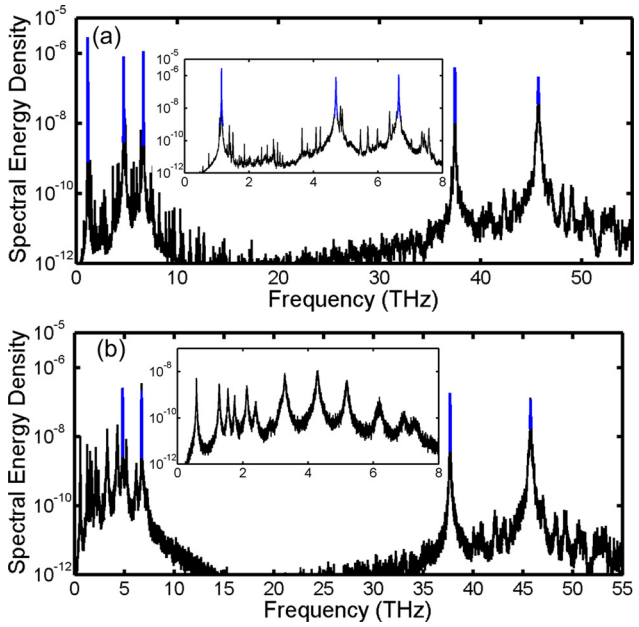

FIG. 5. Semilogarithmic plot (black line) of the SED along the Γ-M direction at $q^* = 2/14$. The blue lines show the fitting curves to Lorentzian function. (a) Isolated single layer graphene (SLG); the inset shows ZA, TA, and LA modes in the region below 8 THz. (b) Supported SLG; the inset shows the modes corresponding to out-of plane vibrations (including ZA mode) in the region below 8 THz.

profiles. Since, the SLG have 28 unit cells in the x direction in our simulations, there are 14 allowed wave vectors in the Γ-M direction of phonon space. Comparing Figs. 5(a) and 5(b), it is observed that the first peak corresponding to ZA mode in isolated SLG (Fig. 5(a)) is highly suppressed in the supported SLG (Fig. 5(b)). Several new peaks corresponding to the out-of-plane vibration modes appear for supported SLG as shown in the inset of Figure 5(b). The intensity of newly created peaks has been significantly diminished for wave vectors larger than 0.5. The ZA mode of the isolated SLG (the first peak in Fig. 5(a)) has the largest magnitude and narrowest width, which indicates a long lifetime (as $\tau = 1/2\gamma$ from Eq. (7)). The magnitude of SED of ZA mode in supported SLG is more than 2 orders smaller than that of isolated SLG. The life time of ZA mode of isolated SLG is in the range of 12 ps to 165 ps; relatively long life time is observed in the small wave vector region. The suppressed ZA modes of supported SLG have a lifetime below 17 ps for all the allowed wave vectors. The newly created phonon modes due to the substrate scattering have small life time as well as small group velocities (as shown in the inset of Fig. 4(b)), which indicates a negligible contribution to the thermal transport. The TA and LA modes have relatively small phonon life time, 4 ps − 43 ps for the isolated SLG and 1.5 ps − 20 ps for the supported SLG.

The contribution of different phonon modes to thermal conductivity of isolated and supported SLGs ($\chi = 1$) is listed in Table I. The classical definition of phonon specific heat is $C_{ph} = k_B$. We calculate the mode contribution using both the classical and quantum definitions of C_{ph}. The contributions from the small wave vector region, $q^* < 0.5$, are also presented in Table I in brackets next to the total contribution. Even though ZA modes have a relatively long life time in the low wave vector region, the corresponding contribution to thermal conductivity is small (21% for isolated SLG) due to the small group velocity of ZA modes in this regime. The three optical modes also have small group velocity as well as little contribution to the thermal conductivity. The peaks for ZA mode of supported SLG are difficult to locate out of those newly appearing modes from the semilogarithmic plot of SED for the wave vectors q* below 0.5. So, we do not fit the SED profiles of ZA modes for $q^* < 0.5$, and neglect the corresponding contribution to the thermal conductivity. This can be justified as the ZA modes have small contribution in this region due to small group velocity in addition to the large suppression of these modes in supported SLG.

Referring to Table I, it is observed that the contributions from LA, out-of-plane optical (ZO), longitudinal optical (LO), transverse optical (TO) modes to the thermal conductivity are reduced by at least 50% when the quantum definition of C_{ph} is used. This is because the quantum definition gives a small value of C_{ph} at high frequency region due to the low phonon population and major contributions to LA, ZO, LO, and TO modes come from high frequency region. Table I shows the thermal conductivity estimations using classical definition of C_{ph} is in good agreement with the Green-Kubo results for both isolated and supported SLGs. This is comprehensible as the thermal conductivity predictions using Green-Kubo method is done using classical EMD results. The reduction in total thermal conductivity due to the substrate scattering is 28.1% using the classical definition of C_{ph}, which is also in good agreement with the Green-Kubo method. The contributions from the three acoustic modes (ZA, TA, and LA) dominate the thermal conductivity for both isolated and supported SLGs. In isolated SLG, the LA, TA, and ZA phonons contribute 654.2, 330.5, and 361.9 W/mK, respectively. The contribution of LA phonons is about 40% at the room temperature while TA and ZA phonons contribute 20% and 22%, respectively. The study in Ref. 29 showed the contributions of 50% and 49% from LA and TA phonons and

TABLE I. The mode contribution to thermal conductivity of isolated single layer graphene (SLG) and supported SLG ($\chi = 1$). The values in the brackets are the contributions from the small wave vector region ($q^* < 0.5$).

Phonon mode		ZA (W/mK)	TA (W/mK)	LA (W/mK)	ZO (W/mK)	LO (W/mK)	TO (W/mK)	Total (W/mK)
Classical C_{ph}	Isolated SLG	361.9 (77.5)	330.5 (198.1)	654.2 (303.1)	180.5 (25.4)	73.2 (0.8)	6.5 (1.3)	1606.7 (606.6)
	Supported SLG	79.9 (N/A)	247.6 (126.6)	576.8 (232.9)	155.4 (29.0)	88.1 (0.6)	7.0 (1.8)	1154.8 (390.9)
Quantum C_{ph}	Isolated SLG	314.1 (76.0)	240.2 (171.0)	310.7 (225.7)	34.0 (2.9)	4.7 (0.0)	0.3 (0.0)	903.9 (475.7)
	Supported SLG	63.7 (N/A)	168.8 (107.1)	247.3 (172.8)	29.3 (3.3)	5.6 (0.0)	0.3 (0.1)	514.9 (283.3)

negligible contribution from the rest of phonons at T = 400 K. In the SLG supported on Cu, the ZA modes have been highly suppressed due to the substrate scattering. The reduction in ZA mode contribution is about 282 W/mK (78%) and 250 W/mK (80%) for the classical and quantum definitions of C_{ph}, respectively. As indicated in Figs. 5(b), the ZA phonons below 6 THz ($q^* \leq 0.5$) have been suppressed, but their contributions are only 77.5 W/mK (see Table I) which are much smaller than the total reduction in ZA mode contribution. This suggests that the phonon lifetimes of ZA phonons above 6 THz ($q^* > 0.5$) are also significantly reduced due to the interaction with the substrate. The thermal conductivities of LA and TA phonons decrease by 12% and 25% for the classical definition of C_{ph}. However, as the contributions of the LA and TA phonons are large in the isolated SLG, the absolute value of their reduction is comparable to that of ZA phonons.

IV. CONCLUSIONS

In summary, we studied the contribution of different phonon modes to the thermal conductivity of both isolated and Cu supported SLGs using equilibrium MD simulations. While using the classical definition of specific heat, the results from the Green-Kubo and RTA methods are in good agreement for both isolated and supported SLGs. The analysis using Green-Kubo method shows a thermal conductivity reduction of 28%–44% due to the substrate scattering which strongly depends on the interaction strength between C and Cu atoms. The thermal transport in the isolated SLG is dominated by the three acoustic modes, the LA, TA, and ZA phonon modes which contribute 654.2, 330.5, and 361.9 W/mK to lattice thermal conductivity, respectively. The interaction with Cu-substrate results in several new phonon modes but with negligible contribution to the thermal conductivity as they have small group velocities and life time. The thermal conductivity contributions of LA, TA, and ZA phonons are reduced by 12%, 25%, and 78%, respectively, due to the interaction with Cu substrate. The reduction in phonon thermal conductivity of SLG supported on different metals or dielectric materials will be different as interfacial interaction strongly depends on the bonding and structure at the interface.

[1]K. I. Bolotin, K. J. Sikes, Z. Jiang, M. Klima, G. Fudenberg, J. Hone, P. Kim, and H. L. Stormer, Solid State Commun. **146**, 351 (2008).
[2]A. H. Castro Neto, F. Guinea, N. M. R. Peres, K. S. Novoselov, and A. K. Geim, Rev. Mod. Phys. **81**, 109 (2009).
[3]J. H. Seol, I. Jo, A. L. Moore, L. Lindsay, Z. H. Aitken, M. T. Pettes, X. S. Li, Z. Yao, R. Huang, D. Broido, N. Mingo, R. S. Ruoff, and L. Shi, Science **328**, 213 (2010).
[4]A. A. Balandin, Nature Mater. **10**, 569 (2011).
[5]M. Freitag, M. Steiner, Y. Martin, V. Perebeinos, Z. H. Chen, J. C. Tsang, and P. Avouris, Nano Lett. **9**, 1883 (2009).
[6]S. Ghosh, I. Calizo, D. Teweldebrhan, E. P. Pokatilov, D. L. Nika, A. A. Balandin, W. Bao, F. Miao, and C. N. Lau, Appl. Phys. Lett. **92**, 151911 (2008).
[7]A. A. Balandin, S. Ghosh, W. Z. Bao, I. Calizo, D. Teweldebrhan, F. Miao, and C. N. Lau, Nano Lett. **8**, 902 (2008).
[8]S. S. Chen, Q. Z. Wu, C. Mishra, J. Y. Kang, H. J. Zhang, K. J. Cho, W. W. Cai, A. A. Balandin, and R. S. Ruoff, Nature Mater. **11**, 203 (2012).
[9]W. W. Cai, A. L. Moore, Y. W. Zhu, X. S. Li, S. S. Chen, L. Shi, and R. S. Ruoff, Nano Lett. **10**, 1645 (2010).
[10]B. W. Li, Z. Q. Wang, R. G. Xie, C. T. Bui, D. Liu, X. X. Ni, and J. T. L. Thong, Nano Lett. **11**, 113 (2011).
[11]P. L. McEuen, X. D. Xu, N. M. Gabor, J. S. Alden, and A. M. van der Zande, Nano Lett. **10**, 562 (2010).
[12]E. Pop, Nano Res. **3**, 147 (2010).
[13]M. H. Bae, Z. Y. Ong, D. Estrada, and E. Pop, Nano Lett. **10**, 4787 (2010).
[14]A. D. Liao, J. Z. Wu, X. R. Wang, K. Tahy, D. Jena, H. J. Dai, and E. Pop, Phys. Rev. Lett. **106**, 256801 (2011).
[15]F. Schwierz, Nat. Nanotechnol. **5**, 487 (2010).
[16]T. H. Yu, C. W. Liang, C. Kim, E. S. Song, and B. Yu, IEEE Electron Device Lett. **32**, 1110 (2011).
[17]Q. Shao, G. Liu, D. Teweldebrhan, and A. A. Balandin, Appl. Phys. Lett. **92**, 202108 (2008).
[18]W. J. Evans, L. Hu, and P. Keblinski, Appl. Phys. Lett. **96**, 203112 (2010).
[19]L. Lindsay and D. A. Broido, Phys. Rev. B **81**, 205441 (2010).
[20]J. N. Hu, S. Schiffli, A. Vallabhaneni, X. L. Ruan, and Y. P. Chen, Appl. Phys. Lett. **97**, 133107 (2010).
[21]J. D. Gale and A. L. Rohl, Mol. Simul. **29**, 291 (2003).
[22]S. Plimpton, J. Comput. Phys. **117**, 1 (1995).
[23]L. Lindsay, D. A. Broido, and N. Mingo, Phys. Rev. B **82**, 115427 (2010).
[24]L. Lindsay, D. A. Broido, and N. Mingo, Phys. Rev. B **83**, 235428 (2011).
[25]D. L. Nika, E. P. Pokatilov, A. S. Askerov, and A. A. Balandin, Phys. Rev. B **79**, 155413 (2009).
[26]D. Singh, J. Y. Murthy, and T. S. Fisher, J. Appl. Phys. **110**, 044317 (2011).
[27]P. G. Klemens, Int. J. Thermophys. **22**, 265 (2001).
[28]B. D. Kong, S. Paul, M. B. Nardelli, and K. W. Kim, Phys. Rev. B **80**, 033406 (2009).
[29]D. L. Nika, S. Ghosh, E. P. Pokatilov, and A. A. Balandin, Appl. Phys. Lett. **94**, 203103 (2009).
[30]D. L. Nika, E. P. Pokatilov, and A. A. Balandin, Phys. Status Solidi B **248**, 2609 (2011).
[31]D. Singh, J. Y. Murthy, and T. S. Fisher, J. Appl. Phys. **110**, 113510 (2011).
[32]Z. P. Xu and M. J. Buehler, J. Phys.: Condens. Matter **22**, 485301 (2010).
[33]G. Giovannetti, P. A. Khomyakov, G. Brocks, V. M. Karpan, J. van den Brink, and P. J. Kelly, Phys. Rev. Lett. **101**, 026803 (2008).
[34]S. M. Foiles, M. I. Baskes, and M. S. Daw, Phys. Rev. B **33**, 7983 (1986).
[35]Z. P. Xu and M. J. Buehler, ACS Nano **3**, 2767 (2009).
[36]Z. Y. Ong and E. Pop, Phys. Rev. B **81**, 155408 (2010).
[37]P. K. Schelling, S. R. Phillpot, and P. Keblinski, Phys. Rev. B **65**, 144306 (2002).
[38]A. J. H. McGaughey and M. Kaviany, in *Advances in Heat Transfer*, edited by J. P. H. A. B.-C. George, A. Greene, and I. C. Young (Elsevier, 2006), Vol. 39, p. 169.
[39]G. Cuniberti, J. Haskins, A. Kinaci, C. Sevik, H. Sevincli, and T. Cagin, ACS Nano **5**, 3779 (2011).
[40]E. S. Landry, M. I. Hussein, and A. J. H. McGaughey, Phys. Rev. B **77**, 184302 (2008).
[41]A. J. H. McGaughey and M. Kaviany, Phys. Rev. B **69**, 094303 (2004).
[42]J. A. Thomas, J. E. Turney, R. M. Iutzi, C. H. Amon, and A. J. H. McGaughey, Phys. Rev. B **81**, 081411 (2010).
[43]D. P. Sellan, E. S. Landry, J. E. Turney, A. J. H. McGaughey, and C. H. Amon, Phys. Rev. B **81**, 214305 (2010).
[44]D. Donadio and G. Galli, Phys. Rev. Lett. **99**, 255502 (2007).
[45]H. Zhang, G. Lee, and K. Cho, Phys. Rev. B **84**, 115460 (2011).
[46]J. Tersoff, Phys. Rev. B **37**, 6991 (1988).